Plasmonics (2011) 6:753–759
DOI 10.1007/s11468-011-9260-1

All-Optical Plasmonic Switches Based on Coupled Nano-disk Cavity Structures Containing Nonlinear Material

Jin Tao · Qi Jie Wang · Xu Guang Huang

Received: 26 May 2011 / Accepted: 28 July 2011 / Published online: 9 August 2011

Abstract All-optical plasmonic switches based on a novel coupled nano-disk cavity configuration containing nonlinear material are proposed and numerically investigated. The finite difference time domain simulation results reveal that the single-disk plasmonic structure can operate as an "on–off" switch with the presence/absence of pumping light. We also demonstrate that the proposed T-shaped plasmonic structure with two disk cavities can switch signal light from one port to another under an optical pumping light, functioning as a bidirectional switch. The proposed nano-disk cavity plasmonic switches have many advantages such as compact size, requirement of low pumping light intensity, and ultra-fast switching time at a femto-second scale, which are promising for future integrated plasmonic devices for applications such as communications, signal processing, and sensing.

J. Tao · Q. J. Wang
Division of Microelectronics, School of Electrical and Electronic Engineering, Nanyang Technological University, Nanyang 639798, Singapore

Q. J. Wang (✉)
Division of Physics and Applied Physics, School of Physical and Mathematical Sciences, Nanyang Technological University, Nanyang 639798, Singapore
e-mail: qjwang@ntu.edu.sg

X. G. Huang
Key laboratory of Photonic Information Technology of Guangdong Higher Education Institutes, South China Normal University, Guangzhou 510006, China

Keywords All-optical switch · Surface plasmon · Waveguide · Photonic integrated circuits

Introduction

Photonic components are superior to the electronic ones in term of the operational bandwidth, but the diffraction limit of light poses a significant challenge to the miniaturization and ultra-density integration of optical circuits [1]. Plasmonic devices, based on surface plasmon-polaritons (SPPs) propagating at metal–dielectric interfaces, have shown great potential to guide and manipulate light by metallic nano-structures at deep sub-wavelength scales [2]. Various passive plasmonic components have been demonstrated by numerical simulations and/or experiments, such as couplers [3], Bragg grating reflectors [4], Mach-Zehnder interferometers, ring resonators [5, 6], tooth-shaped waveguide filters [7–10], and plasmonic collimators[11–14]. However, to achieve active control of optical signals in nano-scale SPPs devices is still one of the remaining challenges.

Recently, some methods for active plasmonic devices have been proposed, such as thermo-optic mechanism [15], absorption activation by quantum dots [16], electro-optic mechanism [17, 18], adoption of photo-chromic molecules [19], and exploration of nonlinear effects [20, 21]. Among these, using optical nonlinear effects is an attractive approach for active control of optical signal in plasmonic devices because those nonlinear materials can be operated in an all-optical means with an ultra-fast response time. Some all-optical bistable switches have been proposed [22, 23]; these structures have large sizes over several micrometers

with large period numbers and can only realize single-directional "on–off" switching function.

In this paper, we propose compact nano-scale all-optical plasmonic switches based on coupled nano-disk cavity structures. The transmission response of a single nano-disk cavity structure is first studied. The single-disk cavity structure filled with optical nonlinear materials can be treated as an "on–off" switch in which the transmission can be modulated "on–off" with an external pumping beam. As an extension to the single-disk structure, a bidirectional switch based on a T-shaped disk cavities structure is demonstrated. The finite difference time domain (FDTD) method is used in simulations [24]. The performance of the proposed devices has great advantages of small size, requirement of low pumping light intensity, and ultra-fast response time that have potential applications in ultra-compact all-optical integrated photonic circuits.

The Transmission Response of the Single Nano-disk Cavity Structure

We first investigate the transmission characteristics of a single nano-disk structure shown in Fig. 1a, which is consisted of a sub-wavelength metal–dielectric–metal (MDM) waveguide side-coupled to a disk cavity, where w and R stand for the width of the bus waveguide and the radius of the disk cavity, respectively. G denotes the gap distance between the bus waveguide and the disk cavity. The metal is assumed to be silver. Its dielectric constant is taken from the experimental data in [25], including both the real and the imaginary parts. And the dielectric in the bus waveguide and nano-disk cavity is assumed to be air with a refractive index n_0=1.

The single nano-disk cavity in the structure behaves as a resonant cavity and supports a resonant mode at a frequency of w_0 (corresponding to a resonant wavelength λ_0). Using the temporal coupled theory [26], the transmission and reflection coefficients of the structure are described, respectively, as:

$$T(\omega) = \frac{(\omega-\omega_0)^2 + (1/\tau_i)^2}{(\omega-\omega_0)^2 + (1/\tau_i + 1/\tau_e)^2} \quad (1)$$

$$R(\omega) = \frac{(1/\tau_e)^2}{(\omega-\omega_0)^2 + (1/\tau_i + 1/\tau_e)^2} \quad (2)$$

Where ω is the frequency of the incident wave, and ω_0 the frequency at resonance, $1/\tau_i$ is the decay rate of the field due to the internal loss in the disk cavity. $1/\tau_e$ is the decay rate due to the power escape through the waveguide. From Eqs. 1 and 2, it is found that the transmission and reflection spectra exhibit Lorentzian line shape. At the resonance frequency ω_0, the incident power is reflected and results in a transmission notch with a minimal value of $(1/\tau_i)^2/(1/\tau_i+1/\tau_e)^2$ and reflection peak with a maximum value of $(1/\tau_e)^2/(1/\tau_i+1/\tau_e)^2$. For frequency of the incident wave far from the resonance frequency, the cavity mode is not excited and therefore transmits through the bus waveguide. The filtering performance of the structure can be explained as follows, the incident SPP wave passing through the bus waveguide is partly coupled to the mode in the nano-disk cavity. The mode begins to resonant in the cavity. After being partly decoupled into the bus waveguide in each resonant cycle, it interferes with the modes in the bus waveguide. The resonant wavelength is determined by the resonance condition of the cavity $2\pi \cdot R_{\text{eff}} \cdot N_{\text{eff}} = m\lambda$, where

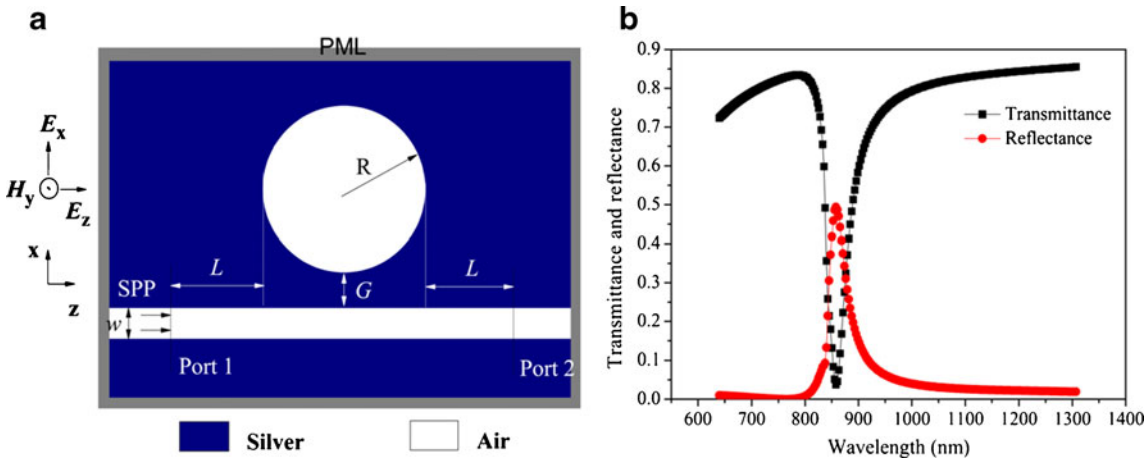

Fig. 1 **a** Schematic structure of the single nano-disk cavity structure where a nano-disk is coupled to a bus waveguide. **b** Corresponding transmission and reflection spectra of the single nano-disk cavity structure with R=210 nm and G=10 nm. Absorption of surface plasmons by the metal (*silver*) is considered in the simulation

R_{eff} is the effective radius and N_{eff} is the effective refractive index in the cavity which increases with the increase of the dielectric index n in the cavity [27].

A two-dimension FDTD method is used to study the properties of the single-disk cavity structure, with the perfectly matched layer absorbing boundary conditions at all boundaries of the simulation domain. Since the width of the bus waveguide is much smaller than the operating wavelength in the structure, only the fundamental waveguide mode is supported. The incident light for excitation of the SPP mode is a TM-polarized (the magnetic field is parallel to y axis) fundamental mode. In the following FDTD simulations, the grid size in the x and the z directions are chosen to be $\Delta x=\Delta z=5$ nm and $\Delta t=\Delta x/2c$, which are sufficient for the numerical convergence. The width w of the bus waveguide is set to be 50 nm while the length of L is fixed to 250 nm. A typical transmission and reflection spectra of the coupled disk cavity structure with $R=210$ nm and gap $G=10$ nm is shown in Fig. 1b. One can see that there is a sharp transmission notch with minimum transmittance 2% at the resonant wavelength of 858 nm. The full width at half maximum of the notch is 40 nm. The intensity of the reflection peak does not reach unity due to the internal loss from the silver in the nano-cavity. At resonance, if there is no internal loss in the cavity ($1/\tau_i=0$) the incident mode is completely reflected and the spectral width of the resonance is determined by the coupling between the bus waveguide and nano-disk cavity. The coupling strength is stronger, the Q factor of the structure is much higher.

Figure 2a shows the transmission spectra of the single air-coupled disk cavity structure in a notch filter characteristic with different radii of R. It reveals that the central wavelength of the notch moves to a long wavelength with the increase of R. Figure 2b reveals that the central wavelength of the notch has a linear relationship with the radius of the nano-disk cavity as expected in resonance condition. Figure 3a shows the transmission spectra of the coupled disk cavity with different dielectric refractive indexes at a fixed radius of 170 nm. One can see that the wavelength of the notch has a red-shift and the maximum transmittance of the non-resonant wavelength can reach 80%. From Fig. 3b, it is found that the red-shift of the wavelength of the notch has a linear relationship with the dielectric index of the cavity. Therefore, one can realize the narrow band filtering function at desired wavelengths by properly choosing the parameters of the coupled nano-disk cavity. Next, we will use the transmittance shifting from a lower value to a high value to realize switching functions by actively tuning the refractive index of the material filled in the nano-disk cavity.

All-Optical Switches Based on Coupled Nano-disk Cavities Structures

We consider a silver–dielectric–silver MDM waveguide coupling to a nano-disk cavity filling with a Kerr nonlinear material (Fig. 4a) whose nonlinear refractive index of the material can be tuned with an external control (pumping) beam. The metal–dielectric composite materials are chosen in the structure, because they have a large third-order optical nonlinear susceptibility and ultra-fast response time which are important for switching function. The typical value of the third-order nonlinear susceptibility $\chi^{(3)}$, is up to 10^{-7} esu with a pulse laser duration of 200 fs at the wavelength of 550 nm. In this paper, Au/SiO_2 with $\chi^{(3)}=1.7\times10^{-7}$ esu (2.37×10^{-15} m^2/v^2) [28] is chosen to fill in the disk cavity and the bus waveguide, and the filling materials could be extended to other Kerr nonlinear materials. The refractive index of the nonlinear material Au/SiO_2 can be expressed as $n=n_0+n_2I$, where $n=1.47$ is the linear refractive index, $n_2=2.07\times10^{-9}$ cm^2/W is the nonlinear refractive index coefficient and I is the pumping beam intensity (power per unit area).

Figure 4b exhibits the transmission spectra at two different intensities of the pumping light, at $w=50$ nm, $L=300$ nm, $G=10$ nm, and $R=154$ nm. As can be seen, the

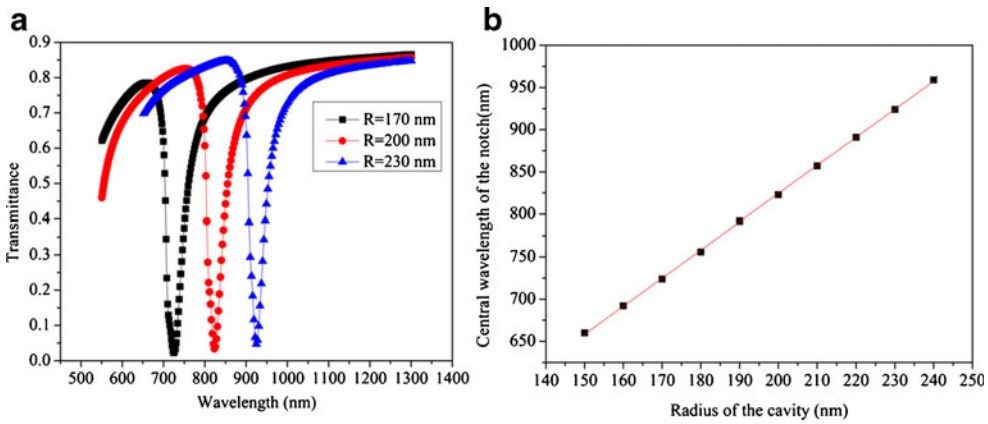

Fig. 2 **a** Transmission spectra of the single air-coupled disk cavity structure with different radii of R. **b** Relationship between the central wavelengths of the notch and the radius of the nano-disk cavity

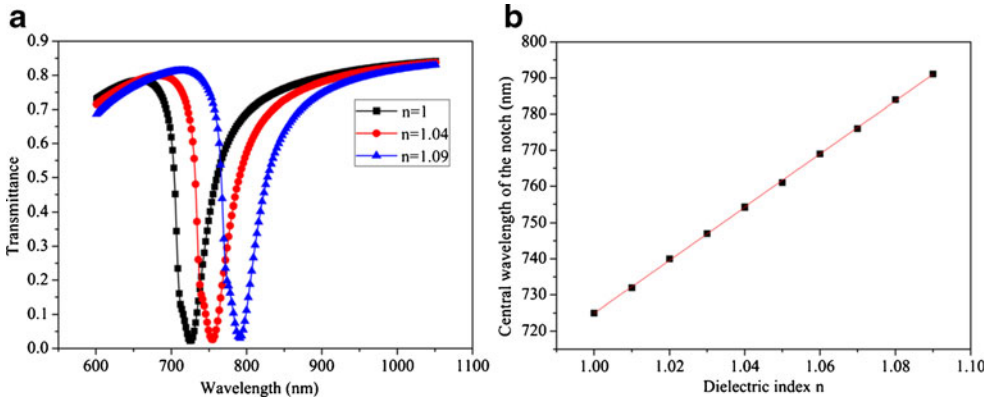

Fig. 3 **a** Transmission spectra of the single-disk cavity structure with different refractive indexes for a fixed radius of 170 nm. The refractive index changes from 1 to 1.09. **b** Relationship between the central wavelength of the notch and the dielectric refractive index in the cavity

transmission of the notch red-shifts from 980 to 1050 nm when pumping intensity I increases from I_0=0 (in the absence of pumping light) to I_1=48.31 MW/cm^2 (with optical pumping, corresponding to 50 mW of optical power), indicating that the central wavelength of the notch can be tuned by the nonlinearity of the Kerr medium in the structure. Without pumping light the light signal of 980 nm is the resonant wavelength and nearly completely reflected. With the optical pumping at 550 nm, the transmittance of signal light at 980 nm increases from 0.02 to 0.73. Thus, the coupled disk cavity structure filled with a nonlinear Kerr material can realize an all-optical switch function, in which the "on/off" states correspond to with/without the optical pumping. The magnetic field profiles of the SPP propagation at the wavelength of 980 nm through the structure are displayed in Fig. 5. Figure 5a shows the "off" state in the absence of pumping light and the SPP wave is completely blocked to the right port. While Fig. 5b shows "on" state in the presence of the optical pumping (intensity I_1=48.31 MW/cm^2) with a transmittance to the right port of nearly 75%, corresponding to an insertion loss of 1.2 dB.

The modulation depth of the single-disk cavity switch is defined as the ratio of the transmittance with the optical pumping to that without the optical pumping, M_s= 10log$_{10}$[$T(I_1)/T(I_0)$]. The modulation depth of the structure as a function of the optical pumping intensities at the signal wavelength of 980 nm is shown in Fig. 6. One can see that the modulation depth increases with the increase of the pump intensity. For a modulation depth of 14.6 dB, a relatively low pump intensity of I_1=48.31 MW/cm^2 is enough. We estimated that the pump power for the "on" state will be on the order of 50 mW and the intensity which are much lower than the result obtained in [29, 30], respectively, when considering to achieve the same the refractive index increments.

The single side-coupled disk cavity structure discussed above can act as an "on–off" all-optical plasmonic switch. However, in some cases, it is necessary to switch optical signal from one port to another port. In Fig. 7, we show a schematic structure of a bidirectional plasmonic switch based on two side-coupled disk cavities structure. The whole structure is comprised of a T-shaped splitter and two nano-disk cavities filled with Kerr nonlinear material Au/SiO_2. The parameters of the structure are chosen as: the input waveguide width w=50 nm, gap G=10 nm, distance L=300 nm, and L_1=L_2=350 nm. Figure 8a shows the transmission spectra at the two ports of the structure with R_1=140 nm and R_2=154 nm. The resonant wavelength of the left nano-disk cavity is designed to be 910 nm, thus the light signal at 910 nm is reflected by the left nano-disk cavity, so there is a peak in the transmission spectra of port 2. Similarly, the resonant wavelength of the right nano-disk

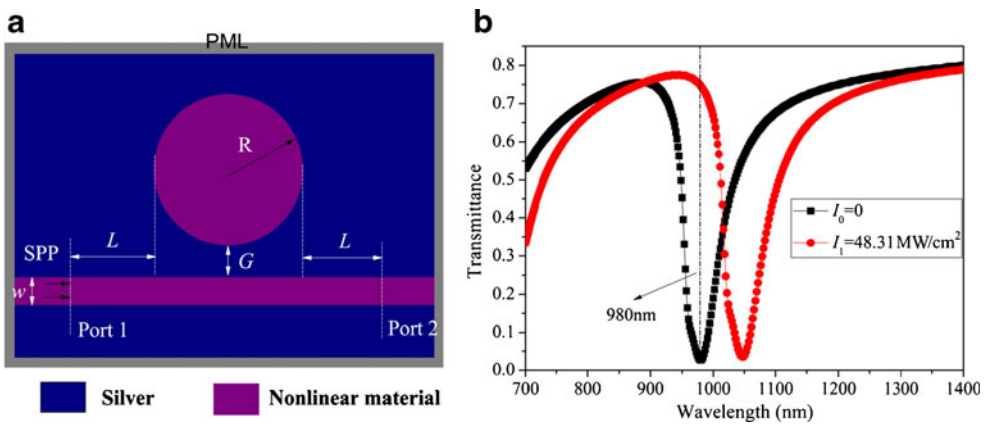

Fig. 4 **a** Schematic structure of a switch consisting of an MDM waveguide coupling to a disk cavity filling with a Kerr material. **b** Transmission spectra of the structure at two different pumping intensities with w=50 nm, L=300 nm, G=10 nm, and R=154 nm

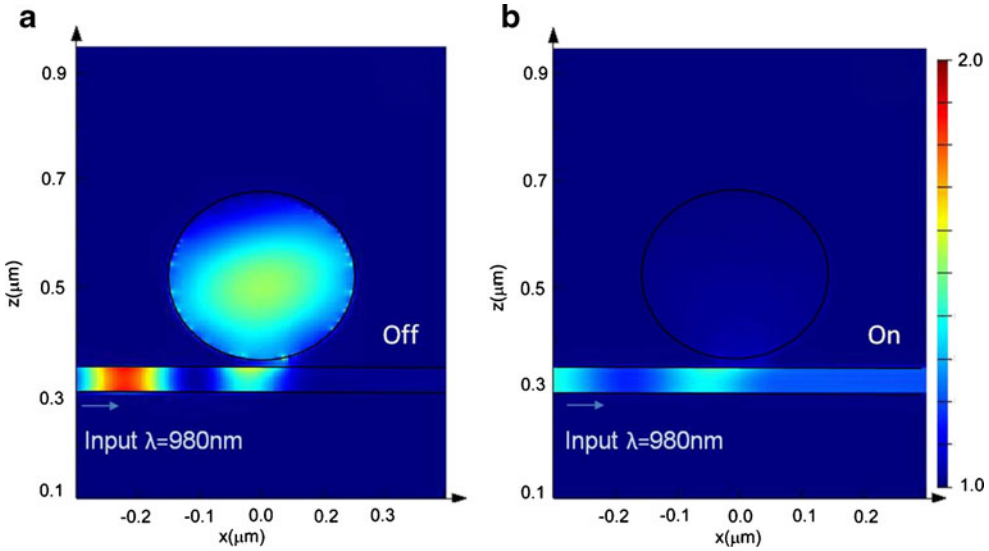

Fig. 5 Simulated magnetic field profiles of the single-disk switch at signal light wavelength of 980 nm. **a** The "*off*" state without the pumping light where no light is transmitted to the right port; and **b** the "*on*" state with the pumping light. The parameters of the structure are the same as those used in Fig. 4

cavity is 980 nm. Light signal at 980 nm is reflected by the port 2, then propagates through port 1. The distance between the bus waveguide and the input waveguide will affect the performance of the switch. Here we set L_1=L_2=350 nm corresponding to the structure shown in Figs. 8 and 9. Without the pumping light, the light signal at 980 nm will be reflected from port 2 by the right-side nano-disk cavity. At the junction of the bus waveguide and the input waveguide, the reflected SPP light signal is divided into two parts: one transmits through port 1 of the bus waveguide and the other passes through the incoming waveguide. The part transmitting through the port 1 will interfere with the incident light passing through the bus waveguide. The phase difference is $\Delta\Phi = 2\pi(2n_{\text{eff}}L + w)/\lambda + \phi$, where n_{eff} is the effective index of bus waveguide, and ϕ is the phase change of the reflected SPP light signal passing through the junction from Port 2 which is small and hard to get its value accurately. Through the simulations, we found that when L_1=L_2=350 nm, the transmission contrast ratio is the maximum. Using L= 350 nm, n_{eff}=2.45 for the wavelength of 980 nm in the bus waveguide, w=50 nm in the equation of phase difference, we have $\Delta\Phi = 3.7\pi + \phi \approx 4\pi$. So the interference between the two waves in the left bus waveguide will be enhanced, and the transmission ratio will be maximized.

Figure 8b shows the transmission spectra of the two nano-disk cavities structure with the optical pumping. It is found that when the pumping intensity is tuned from I_0=0 to I_1=53.1 MW/cm^2, the transmission central wavelength

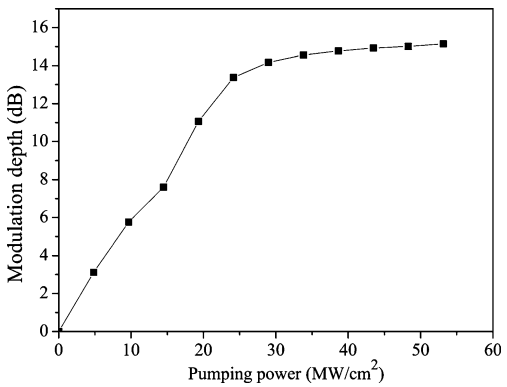

Fig. 6 Modulation depth of the single nano-disk switch as a function of the optical pumping intensity at the signal wavelength of 980 nm. The parameters of the structure are the same as those used in Fig. 4b

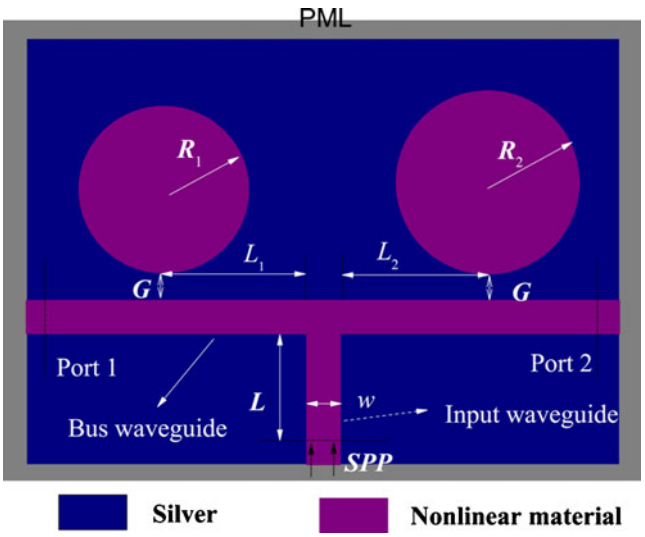

Fig. 7 Schematic structure of a bidirectional all-optical switch based on two side-coupled disk cavities structure

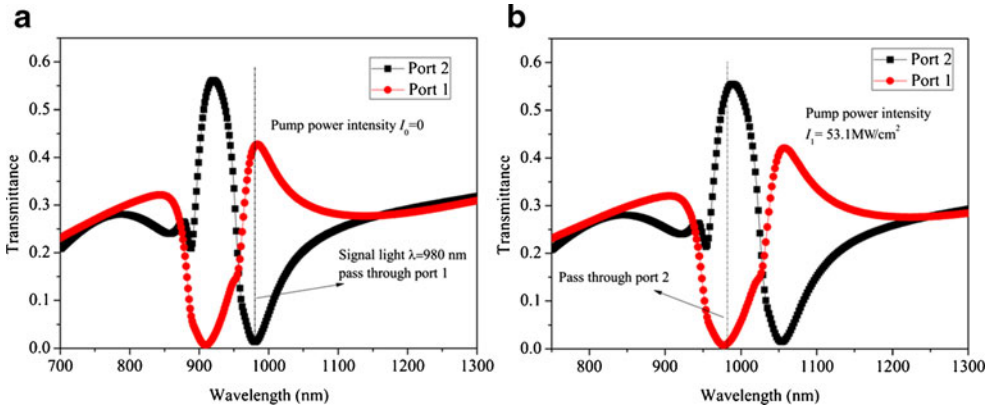

Fig. 8 Transmission spectra of two ports of the T-shaped nano-disk structure at different pumping power levels with R_1=140 nm, R_2=154 nm, and L_1=L_2=350 nm. **a** Without the pumping; **b** with the optical pumping

of the notch of the port 1 red-shifts from 910 to 980 nm and the one of the port 2 shifts from 980 to 1,049 nm. The resonance wavelength of the left nano-disk cavity changes to 980 nm, so the signal light at 980 nm will be reflected from the port 1 and passes through the port 2. The transmission of signal light at 980 nm jumps from 0.013 to 0.555 for the port 2 when the pumping light (532 nm) is increased from 0 to 53.1 MW/cm^2, while the transmittance of the port 1 drops from 0.43 to 0.008. It is clearly seen that the signal light at 980 nm has been directed from the left to the right. Here, we define the transmission contrast ratio of the two ports as M_t=10log$_{10}$ ($T_{1,\ 2}$/$T_{2,\ 1}$). With the optical pumping, the light signal is transferred from the left port 1 to the right port 2 and the transmission contrast ratio is 18.4 dB.

The transmission contrast ratio is not very high is mainly due to the loss in the bus waveguide and nano-disk cavity. One solution to improve the performance of the switch is to combine surface plasmons with electrically and optically pumped gain media such as semiconductor quantum dots [31], semiconductor quantum well, and organic dyes [32] embedded into the structure. Electrically and optically pumped semiconductor gain media and the emerging technology of graphene are expected to provide loss compensation from visible to terahertz spectral range [33].

To clearly observe the bidirectional switching effect, the magnetic fields of the two nano-disk cavities structure are shown in Fig. 9 with/without optical pumping. One can see that the signal light at 980 nm transmits through the port 1 without the pumping (Fig. 9a), and can pass through the port 2 with the pumping (Fig. 9b). The optical Kerr nonlinear material chosen in our structure is metal–dielectric composite material Au/SiO$_2$ which has a large third-order nonlinear susceptibility and ultra-fast response time of 200 fs. Thus, femto-second level switching time of the switches would be achieved in the proposed cavity structures.

Conclusions

In this paper, we have numerically investigated two types of all-optical plasmonic switches based on coupled nano-disk cavity structures filled with optical nonlinear Kerr material.

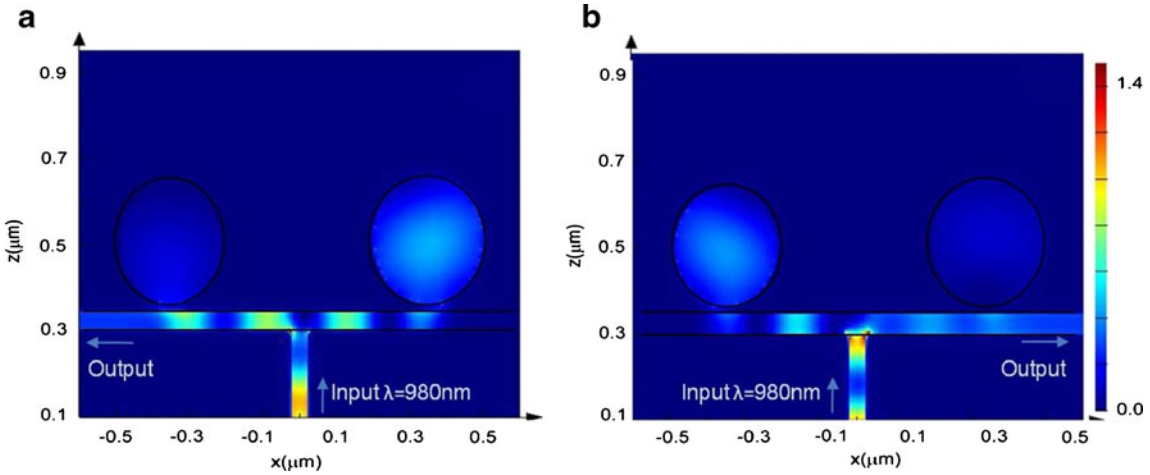

Fig. 9 Simulated magnetic field profiles of the two nano-disk-shaped cavities switch at 980 nm. **a** State of "Left switching" without the pumping (I=0). **b** State of "Right switching" with the pumping (I=53.1 MW/cm^2)

With the active tuning of the pumping light, a single-disk Kerr cavity structure could realize the "on–off" switching function. The T-shaped waveguide coupling to two nano-disk cavities structure could act as a bidirectional switch to switch the incident signal from one port to another. The structures are of small size in the nano-scale, ultra-fast time, requiring lower pumping power. Our structures may open a possibility for future applications in nano-plasmonic information processing and ultra-compact all-optical integration circuits.

Acknowledgments This work is supported by the grant (grant number M58040017) from Nanyang Technological University (NTU), Singapore. Support from the CNRS International-NTU-Thales Research Alliance (CINTRA) Laboratory, UMI 3288, Singapore 637553, is also acknowledged.

References

1. Barnes WL, Dereus A, Ebbsen TW (2003) Surface plasmon subwavelength optics. Nature 424:824–830
2. Gramotnev DK, Bozhevolnyi SI (2010) Plasmonics beyond the diffraction limit. Nature Photonics 4:83–91
3. Zhao H, Guang X, Huang J (2008) Novel optical directional couplers based on surface plasmon polaritons. Physica E 40 (10):3025–3209
4. Hosseini A, Massoud Y (2006) A low-loss metal-insulator-metal plasmonic bragg reflector. Opt Express 14(23):11318–11323
5. Wang TB, Wen XW, Yin CP, Wang HZ (2009) The transmission characteristics of surface plasmon polaritons in ring resonator. Opt Express 17(26):24096–24101
6. Bozhevolnyi SI, Volkov VS, Devaux E, Laluet JY, Ebbesen TW (2006) Channel plasmon subwavelength waveguide components including interferometers and ring resonators. Nature 440:508–511
7. Lin XS, Huang XG (2008) Tooth-shaped plasmonic waveguide filters with nanometeric sizes. Opt Lett 33(23):2874–2876
8. Lin XS, Huang XG (2009) Numerical modeling of a teeth-shaped nanoplasmonic waveguide filter. J Opt Soc Am B 26(7):1263–1268
9. Tao J, Huang XG, Lin XS, Zhang Q, Jin X (2009) A narrow-band subwavelength plasmonic waveguide filter with asymmetrical multiple-teeth-shaped structure. Opt Express 17(16):13989–13994
10. Tao J, Huang XG, Lin XS, Chen JH, Zhang Q, Jin XP (2010) Systematical research on characteristics of double-side teeth-shaped nano-plasmonic waveguide filters. J Opt Soc Am B 27 (2):323–327
11. Yu N, Blanchard R, Fan J, Wang QJ, Plfugl C, Diehl L, Edamura T, Yamanishi M, Kan H, Capasso F (2008) Quantum cascade lasers with integrated plasmonic antenna-array collimators. Opt Express 16:19447
12. Yu N, Wang QJ, Pflugl C, Diehl L, Capasso F, Edamura T, Furuta S, Yamanishi M, Kan H (2009) Semiconductor lasers with integrated plasmonic polarizer. Appl Phys Lett 94:151101
13. Yu N, Kats M, Pflugl C, Geiser M, Wang QJ, Belkin MA, Capasso F, Fischer M, Wittmann A, Faist J, Edamura T, Furuta S, Yamanishi M, Kan H (2009) Multi-beam multi-wavelength semiconductor lasers. Appl Phys Lett 95:161108
14. Yu N, Wang QJ, Kats MA, Fan JA, Khanna SP, Li L, Davies AG, Linfield EH, Capasso F (2010) Designer spoof surface plasmon structures collimate terahertz laser beams. Nat Mater 9:730–735
15. Lereu AL, Passian A, Goudonnet JP, Thundat T, Ferrell TL (2005) Optical modulation processes in thin films based on thermal effects of surface plasmons. Appl Phys Lett 86:154101
16. Pacifici D, Lezec HJ, Atwater HA (2007) All-optical modulation by plasmonic excitation of CdSe quantum dots. Nature Photonic 1:402–406
17. Dicken MJ, Sweatlock LA, Pacifici D, Lezec HJ, Bhattacharya K, Atwater HA (2008) Electroopt modulation in thin film barium titanate plasmonic interferometers. Nano Lett 8:4048–4052
18. Hsiao KS, Zheng YB, Juluri BK, Huang TJ (2008) Light-driven plasmonic switches based on Au nanodisk arrays and photo-responsive liquid crystal. Adv Mater 20:3528–3532
19. Pala RA, Shimizu KT, Melosh NA, Brongersma ML (2008) A nonvolatile plasmonic switch employing photochromic molecules. Nano Lett 8(5):1506–1510
20. Wurtz GA, Zayats AV (2008) Nonlinear surface plasmon polariton polaritonic crystal. Laser Photon Rev 2:125–135
21. Liu YM, Bartal G, Genov DA, Zhang X (2007) Subwavelength discrete solitons in nolinear metamaterials. Phys Rev Lett 99:153901
22. Wurtz GA, Pollard R, Zayats AV (2006) Optical bistability in nonlinear surface-plasmon polaritonic crystals. Phys Rev Lett 97:057402
23. Porto JA, Moreno LM, Garcia-Vidal FJ (2004) Optical bistability in subwavelength slit apertures containing nonlinear media. Phys Rev B 70:081402
24. Schilders WHA, Ciarlet PG, Linons J, Maten EJWT. *Numerical Methods in Electromagnetics* (Elsevier, 2005). In this paper a commercial software Lumerical FDTD solution is used for simulation
25. Palik ED. Handbook of Optical Constant of Solids (Academic, 1985)
26. Haus HA, Lai Y (1992) Theory of Cascaded Quarter wave shifted distributed feedback resonators. IEEE J Quantum Electron 28 (1):205–213
27. Chremmos I (2009) Magnetic field integral equation analysis of interaction between a surface plasmon polariton and a circular dielectric cavity embedded in the metal. J Opt Soc Am A 26:2623–2633
28. Liao HB, Xiao RF, Fu JS, Wang H, Wong KS, Wong GKL (1998) Origin of third-order optical nonlinearity in Au:SiO_2 composite films on femtosecond and picosecond time scales. Opt Lett 23:388–390
29. Al-hemyari K (1993) Ultrafast all-optical switching in GaAlAs directional couplers at 1.55 μm without multiphoton absorption. Appl Phys Lett 63(36):3562
30. Andreas A (2010) Reiserer, Jer-Shing Huang, Bert Hecht, and Tobias Brixner, Subwavelength broadband splitters and switches for femtosecond plasmonic signals, Opt Express 18:11810–11820
31. Plum E, Fedotov VA, Kuo P, Tsai DP, Zheludev NI (2009) Towards the lasing spaser: controlling metamaterial optical response with semiconductor quantum dots. Opt Express 17(10):8548
32. Noginov MA, Zhu G, Mayy M, Ritzo BA, Noginova N, Podolskiy VA (2008) Stimulated emission of surface plasmon polaritons. Phys Rev Lett 101:226806
33. Dubinov A, Aleshkin VY, Mitin V, Otsuji T, Ryzhii V (2011) Terahertz surface plasmons in optical pumped graphene structures. J Phys Condens Matter 23:145302